
Homework 2

To: Andrew Ning
From: Joshua Canlas
Date: February 7, 2020
Subject: Homework 2 Memo

Introduction

The objective of this homework was to find the coefficient of lift, pitching moment, and pressure for a NACA 2412 airfoil using three different methods: thin air foil method, panel method, and CFD. Each section of this report talks about the results that came from each method. The final section provides a brief discussion of the advantages and disadvantages of each method.

1.1 Thin Airfoil Theory

Introduction

The objective of this problem is to find the first three coefficients from the Fourier series, plot c_l and c_{mac} as a function of angle of attack, and plot the c_p distribution where $c_l = 1$.

The thin air foil theory approximates the velocities and pressures on an airfoil using equations that model a combination of point singularities, such as vortices and sources, and the free stream velocity. Since the airfoil is “thin,” the singularities are all modeled at $y = 0$ (not on the edge of the airfoil itself) and the combination of various strength singularities meet to create an accurate model for the airfoil. Additionally, the thin airfoil theory assumes that disturbances are small.

Methods

The first objective of this problem is to solve for the first three Fourier coefficients. This was done using the following equations:

$$A_0 = \alpha - \frac{1}{\pi} \int_0^\pi b(\theta) d\theta$$
$$A_n = \frac{2}{\pi} \int_0^\pi b(\theta) \cos(n\theta) d\theta$$

Conveniently, $b(\theta)$ is found using the Matlab code provided (See Appendix A). The resulting values are displayed in the summary section (see Table 1).

The next objective of this problem is to find both the coefficient of lift, and coefficient of pitching moment about the aerodynamic center as a function of angle of attack. The coefficient of lift and pitching moment about the aerodynamic center are found through the following equations

$$c_L = 2\pi(\alpha - \alpha_0)$$
$$c_{mac} = -\frac{\pi}{4}(A_1 - A_2)$$

where the A coefficients are found using the Fourier coefficient equations shown earlier and

$$\alpha_0 = \frac{1}{\pi} \int_0^\pi b(\theta)(1 - \cos\theta)d\theta$$

As can be seen, the coefficient of lift depends on the angle of attack, while the moment coefficient is not. Therefore, when the coefficient of lift is plotted against angle of attack, it varied, while the moment coefficient remained constant. This plot is shown and discussed in the summary section as well.

The final part of this problem asks for a plot of the coefficient of pressure at the angle of attack when coefficient of lift is equal to 1. The coefficient of lift is found to be approximately equal to 1 when the angle of attack is 8 degrees. Therefore, $\alpha = 8$ for the remainder of this problem, while the freestream velocity is assumed to be $V_\infty = 10$.

To solve for the coefficient of pressure, the induced velocities of the free stream velocity, sources, and vortices must be found for each point. Equations have been created to find the appropriate strength vortices and sources given the specified boundary conditions and parameters used in the problem. These equations find the ideal mix of singularity strengths in order to create the basic airfoil shape so lift and pressure can be accurately modeled.

To begin, the code given to us by Dr. Ning finds the camber line shape of the airfoil, which is necessary since this is where the singularities act according to the thin air foil theory. The provided code then also differentiates to get $d\bar{y}/dx$ and dT/dx . These values, along with the boundary conditions are essential to solving for the source strength in the following equation

$$q(x) = V_\infty \frac{dT}{dx}$$

Since this theory assumes a “thin” airfoil where all singularities are linear functions that act at $y=0$, the following equation finds the velocity magnitude by combining the x and y velocities induced by the freestream velocity (V_∞), sources (u_t, v_t), and vortices (u_c, v_c).

$$V = \sqrt{(V_\infty \cos \alpha + u_t + u_c)^2 + (V_\infty \sin \alpha + v_t + v_c)^2}$$

In order to solve for the velocity, the induced velocities in the x and y direction for each of these three components must be determined.

The induced velocities in the x-direction from the sources are found using the following equation:

$$u_t = \int_0^c \frac{q(s)}{(x-s)} ds$$

where $q(s)$ is the source strength at each point on camber line. The variable x refers to a specific point at which the induced velocities are being summed, while s is a dummy variable that represents an integration along the entire length of the camber line.

Next, the induced velocities in the x-direction from the vortices are found using the following equation:

$$u_c = \pm \frac{\gamma(x)}{2}$$

where,

$$\begin{aligned}\gamma(\emptyset) &= 2V_\infty \left[A_0 \frac{(1 + \cos \emptyset)}{\sin \emptyset} + \sum_n A_n \sin(n\emptyset) \right] \\ A_0 &= \alpha - \frac{1}{\pi} \int_0^\pi b(\theta) d\theta \\ A_n &= \frac{2}{\pi} \int_0^\pi b(\theta) \cos(n\theta) d\theta\end{aligned}$$

Since x was found using \emptyset , the value of $\gamma(x)$ can be found by inserting \emptyset into the equation. The induced velocities in the y-direction caused by the sources and vortices are respectively

$$\begin{aligned}v_t &= \pm \frac{q(x)}{2} \\ v_c &= - \frac{1}{2\pi} \int_0^c \frac{\gamma(s)}{x-s} ds\end{aligned}$$

where $\gamma(s)$ is the vortex strength at each point on the camber line. With each of the induced velocity components determined, the overall velocity at each point on the camber line can now be solved. However, since the thin air foil theory assumes that there are only small disturbances (and there are bound to be large disturbances at the leading edge), Riegel's correction (V_{mod}) can be used to make the results a bit more realistic.

$$V_{mod} = V \frac{1}{\sqrt{1 + \left(\frac{dy}{dx} + \frac{1}{2} \frac{dT}{dx} \right)^2}}$$

We then use this modified velocity distribution to solve for the coefficient of pressure throughout the airfoil

$$c_p = 1 - \left(\frac{V_{mod}}{V_\infty} \right)^2$$

Results and Discussion

Table 1 shows the first three coefficients found in the Fourier series. We used these values to simply confirm that we were solving for the coefficients correctly. The only coefficient that changed when we looked at a different angle of attack was A_0 .

Table 1: First three Fourier coefficients, determined using the Matlab code in appendix A.

Coefficient	Value
A_0	0.0304
A_1	0.0815
A_2	0.0139

Fig. 1 shows a plot for the coefficient of lift and pitching moment about the aerodynamic center as a function of angle of attack. As was mentioned previously, since the aerodynamic center is at the point where the moment does not change with angle of attack, the plot should portray c_{mac} as a constant with varying α while c_l is not. Fig. 1 does indeed show a slightly negative, yet constant coefficient of pitching moment as expected, with a coefficient of lift with a slope of 2π .

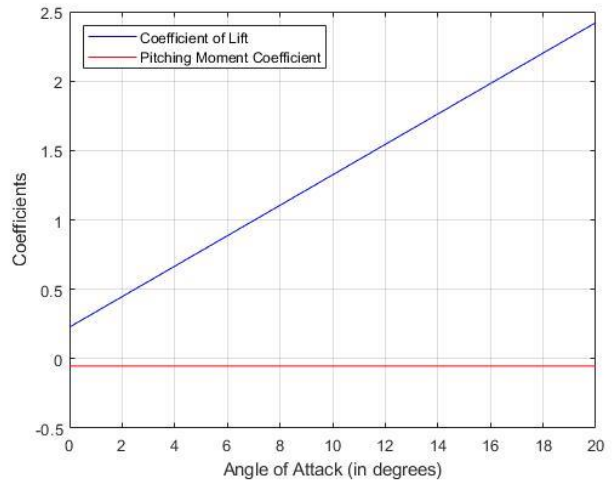


Figure 1: Coefficient of lift and pitching moment plotted for various angles of attack.

Finally, Fig. 2 plots the coefficient of pressure distribution when the angle of attack is equal to 8 (which was determined to be the angle of attack when $c_l = 1$). This plot shows that the pressure coefficient at the leading edge goes to infinity, which is one downside of the thin air foil theory. This occurs because of the small disturbance assumption in thin airfoil theory, which is broken at the leading edge.

2.2 Panel Method

Introduction

The objective of this problem is to plot the convergence of coefficient of lift, coefficient of drag, and coefficient of pitching moment as the number of panels is increased. We were also asked to compare the values found using this method against the thin airfoil theory.

The panel method is similar to the thin air foil method in that it uses a combination of sources, vortices, and the free stream velocity to model an airfoil in order to find the lift and other important values. However, unlike the thin airfoil method, this method places panels to model the airfoil and the singularities are

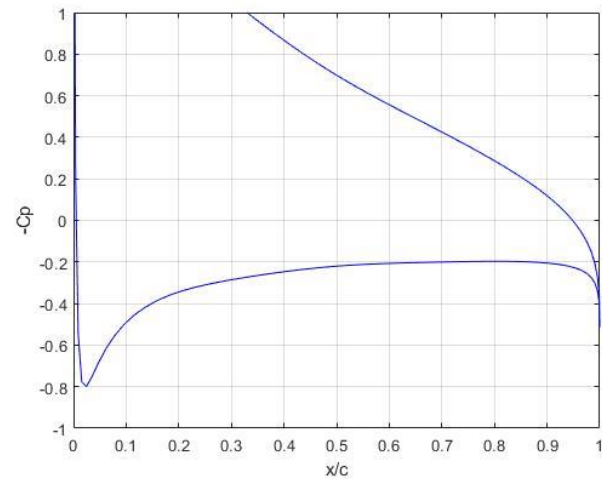


Figure 2: Coefficient of pressure distribution for airfoil at 8 degrees angle of attack. This is where $C_l = 1$.

placed on the panels. The centers of these panels were then evaluated for the induced velocities felt due to the other panels' vortices and sources in combination with the free stream.

Two vital assumptions are made in this solution that must be recognized: the source strength is assumed to be constant across a given panel, while varying from panel to panel, and the vortex strength is constant across all of the panels. All of the code used to solve for the aerodynamic coefficients are found in Appendix B.

Methods

To begin, we created the panels along the airfoil and connected them going clockwise around the airfoil (keeping the body to the right of the panel) and found the center points of each panel.

To solve for the velocities, some simple geometry was first completed to determine the position of the various panels in relation to each other. The following equations were used to relate the distance and angles between panel i (the panel being observed) and panel j (the panel influencing panel i)

$$\begin{aligned}
 r_{ij} &= \sqrt{(\bar{x} - x_j)^2 + (\bar{y} - y_j)^2} \\
 r_{ij+1} &= \sqrt{(\bar{x} - x_{j+1})^2 + (\bar{y} - y_{j+1})^2} \\
 \theta_i &= \tan^{-1} \left(\frac{y_{i+1} - y_i}{x_{i+1} - x_i} \right) \\
 \theta_j &= \tan^{-1} \left(\frac{y_{j+1} - y_j}{x_{j+1} - x_j} \right) \\
 \beta_{ij} &= \begin{cases} \text{atan2} \left(\frac{(x_j - \bar{x}_i)(y_{j+1} - \bar{y}_i) - (y_j - \bar{y}_i)(x_{j+1} - \bar{x}_i)}{(x_j - \bar{x}_i)(x_{j+1} - \bar{x}_i) + (y_j - \bar{y}_i)(y_{j+1} - \bar{y}_i)} \right) & \text{if } i \neq j \\ \pi & \text{if } i = j \end{cases}
 \end{aligned}$$

Next, the source strengths and vortex strength were found using a matrix to combine multiple equations at once as shown below

$$\begin{bmatrix} A_{11} & \cdots & A_{1N} & A_{1,N+1} \\ \vdots & & \vdots & \vdots \\ A_{N1} & \cdots & A_{NN} & A_{N,N+1} \\ A_{N+1,1} & \cdots & A_{N+1,N} & A_{N+1,N+1} \end{bmatrix} \begin{bmatrix} q_1 \\ \vdots \\ q_N \\ \gamma \end{bmatrix} = \begin{bmatrix} b_1 \\ \vdots \\ b_N \\ b_{N+1} \end{bmatrix}$$

where the following equations result from the flow tangency condition ($\vec{V} \cdot \hat{n} = 0$)

$$A_{ij} = \left[\ln \left(\frac{r_{ij+1}}{r_{ij}} \right) \sin(\theta_i - \theta_j) + \beta_{ij} \cos(\theta_i - \theta_j) \right]$$

$$A_{iN+1} = \sum_{j=1}^N \left[\ln \left(\frac{r_{ij+1}}{r_{ij}} \right) \cos(\theta_i - \theta_j) - \beta_{ij} \sin(\theta_i - \theta_j) \right]$$

$$b_i = 2\pi V_\infty \sin(\theta_i - \alpha)$$

Similarly, the following equations result from the Kutta condition

$$\begin{aligned} A_{N+1,j} &= \sum_{k=1 \text{ and } N} \left[\beta_{kj} \sin(\theta_k - \theta_j) - \ln \left(\frac{r_{kj+1}}{r_{kj}} \right) \cos(\theta_k - \theta_j) \right] \\ A_{N+1,N+1} &= \sum_{k=1 \text{ and } N} \left(\sum_{j=1}^N \left[\beta_{kj} \cos(\theta_k - \theta_j) + \ln \left(\frac{r_{kj+1}}{r_{kj}} \right) \sin(\theta_k - \theta_j) \right] \right) \\ b_{N+1} &= -2\pi V_\infty [\cos(\theta_1 - \alpha) + \cos(\theta_N - \alpha)] \end{aligned}$$

Using these two conditions the entire matrix can be solved for q_n and γ . These values are then inserted into the tangential velocity equation.

$$\begin{aligned} V_{ti} &= V_\infty \cos(\theta_i - \alpha) \\ &+ \frac{1}{2\pi} \sum_{j=1}^N \left[q_j \left(\beta_{ij} \sin(\theta_i - \theta_j) - \ln \left(\frac{r_{ij+1}}{r_{ij}} \right) \cos(\theta_i - \theta_j) \right) \right] \\ &+ \frac{\gamma}{2\pi} \sum_{j=1}^N \left[\beta_{ij} \cos(\theta_i - \theta_j) + \ln \left(\frac{r_{ij+1}}{r_{ij}} \right) \sin(\theta_i - \theta_j) \right] \end{aligned}$$

This velocity was then used to find the coefficient of pressure using the following equation:

$$C_p(\bar{x}_i, \bar{x}_j) = 1 - \left(\frac{V_{ti}}{V_\infty} \right)^2$$

Next, the coefficient of lift was found using this equation:

$$c_L = \frac{L'}{\frac{1}{2} \rho v^2 A}$$

$$L' = \rho V_\infty \times \Gamma$$

where the total circulation is found to be

$$\Gamma = \int_0^c \gamma(s) ds$$

The coefficient of pitching moment was found using the following equation:

$$c_m = \frac{M'}{\frac{1}{2}\rho v^2 Ac}$$

The moment is determined by finding the moment arms and forces on each panel caused by the pressure at the center points of each panel. Therefore, the equation for M' can be found using the following equation:

$$M' = \sum_0^n \mathbf{F}_p \times \mathbf{r}_{ac}$$

Results and Discussion

Fig. 3 shows the coefficient of pressure distribution across the chord of the airfoil at an angle of attack of 8 degrees for both the thin airfoil and panel methods. This comparison highlights the limitations of thin air foil theory at the leading edge as it goes to infinity due to the large disturbance that breaks the small disturbance assumption. In contrast, the panel method curve shows a finite upper limit that can be more easily compared to CFD as seen in Problem 2.3.

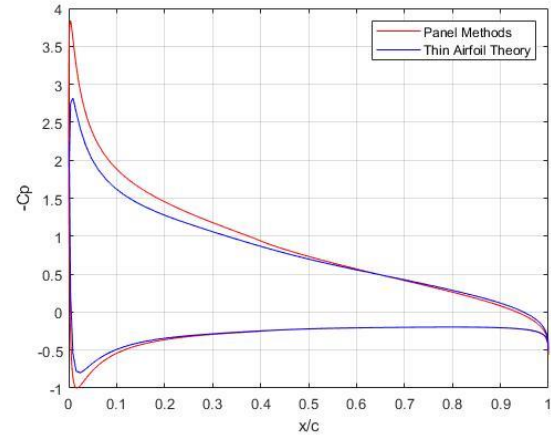


Figure 3: Coefficient of pressure distributions at an angle of attack of 8 degrees for both thin airfoil theory and panel method.

The comparison of coefficients of lift and pitching moment for the thin airfoil method and panel method are shown in Fig. 4. As can be seen, the lines representing the thin airfoil method are very similar to the values found using two different angles of attack in the panel method. This shows that despite having a large disturbance, the thin airfoil and panel methods result in very similar values for coefficient of lift and pitching moment with changing angles of attack.

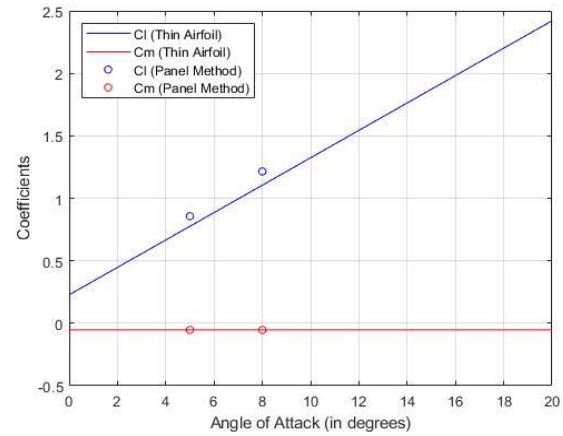


Figure 4: Comparison of coefficient of lift and pitching moment for the thin airfoil theory and panel method.

Finally, Fig. 5 shows the convergence for coefficients of pitching moment, lift, and drag as the number of panels is increased. As can be seen in the figure, using 400 panels results in a relative convergence for all three coefficients such that

the resulting values are not dependent on the number of panels (which makes the solutions more accurate).

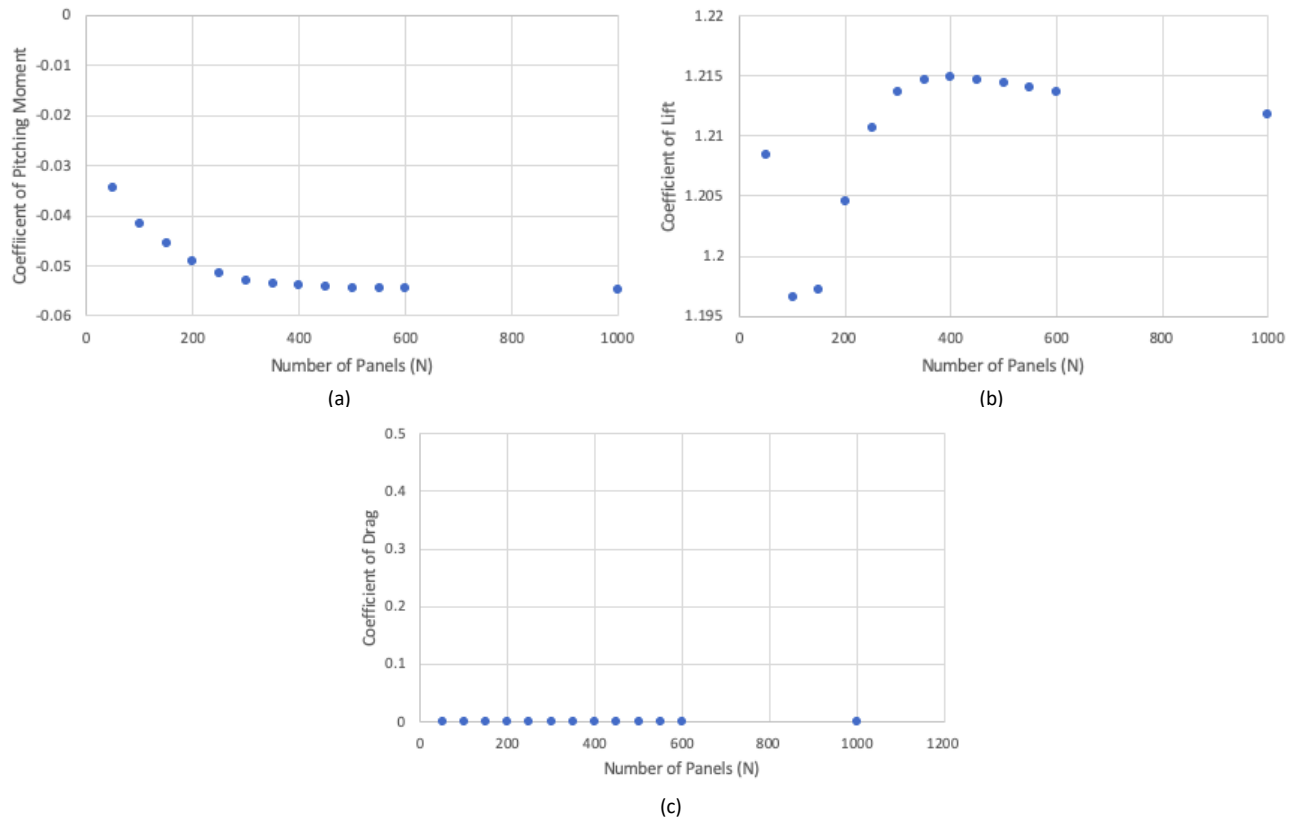


Figure 5: Convergence plots for coefficients of (a) pitching moment about the aerodynamic center, (b) lift, (c) and drag.

2.3 Computational Fluid Dynamics

Introduction

The objective of this problem is to compare the coefficients of lift, pitching moment about the aerodynamic center, and pressure distribution at two different angles of attack for a NACA 2412 airfoil, similar to problems 2.1 and 2.2. In the first homework, a NACA 2412 airfoil was modeled at an angle of attack of 5 degrees. Therefore, the three desired results were plotted using the previously completed analysis, before the angle of attack was changed to 8 degrees and the model was resolved.

The steps taken to update the previous analysis are detailed in the methods section below, while the steps completed in homework 1 are included in Appendix C.

Methods

The only required update from the previously completed analysis, is a change in angle of attack, as well as the addition of an extra plot for the moment about the aerodynamic center and pressure. To change the angle of attack, the entire body could be placed at an angle relative to the free stream velocity, or the free stream velocity could be entered at the angle of attack. The second of these options is used, and therefore the initial velocity conditions are updated as follows:

$$u_i = 10 * \cos (8)$$

$$v_i = 10 * \sin (8)$$

Additionally, the report for lift is updated to read perpendicular to the free stream velocity using sine and cosine as well. Since the moment about the aerodynamic center does not change with angle of attack, this plot does not need to be changed with angle of attack.

To add a plot for the moment about the aerodynamic center, a new x-y plot is added, and the option “moment” is chosen. Since the airfoil will have a moment trying to push down on the front of the airfoil, the moment is defined to be rotating in the positive z direction, at $x = \frac{c}{4}$ which is where the aerodynamic center is located on the body that was chosen (the airfoil).

Another report is then added to display the coefficient of pressure across varying x values. The gauge pressure is set to zero and the density set to 1.225 kg/m³, as was done in homework 1.

Various mesh sizes are then used to find the base size at which the results converged (similar to homework 1). This ensures that the values reported for each of the desired areas are accurate and not mesh dependent. The base size was set to multiple values ranging from 1 to 0.05 (See Appendix C for images of the various mesh images and converging data). The lift, moment, and pressure values all converged by a base size of 0.05.

The lift force and pitching moment are then taken from the reports and entered into an excel spreadsheet that records the force of lift and pitching moment, as well as the base size used to compute them. The force and moments are then converted into coefficients of lift and pitching moment using the following two equations:

$$C_l = \frac{l}{\frac{1}{2} \rho A v^2}$$

$$C_{mac} = \frac{m}{\frac{1}{2} \rho A v^2 c}$$

In these equations, density is 1.225 kg/m³, the area is 1 m² and the velocity is 10 m/s. These coefficients are then recorded so a comparison at $\alpha = 5$ and $\alpha = 8$ can be performed.

Results and Discussion

The results in Table 2 show the change in coefficient of lift and pitching moment about the aerodynamic center at two different angles of attack. The coefficient of lift changes dramatically while the pitching moment coefficient does not, which matches analytical expectations. In fact, the change in C_{mac} is

Table 2: Coefficient of lift and pitching moment determined at two different angles of attack using Star CCM.

Angle of Attack	5°	8°
CL	0.8195918	1.1606531
Cmac	-0.0599837	-0.0636735

attributed mostly to error and slight mesh dependency since the pitching moment about the aerodynamic center should remain the same despite a change in angle of attack.

Fig. 5 then shows the coefficient of pressure distribution across the airfoil for $\alpha = 8$. When the angle of attack is set to 5 the coefficient of pressure drops to a low of only nearly -2, while when the angle of attack is set to 8 the coefficient of pressure drops to a low of about -4.

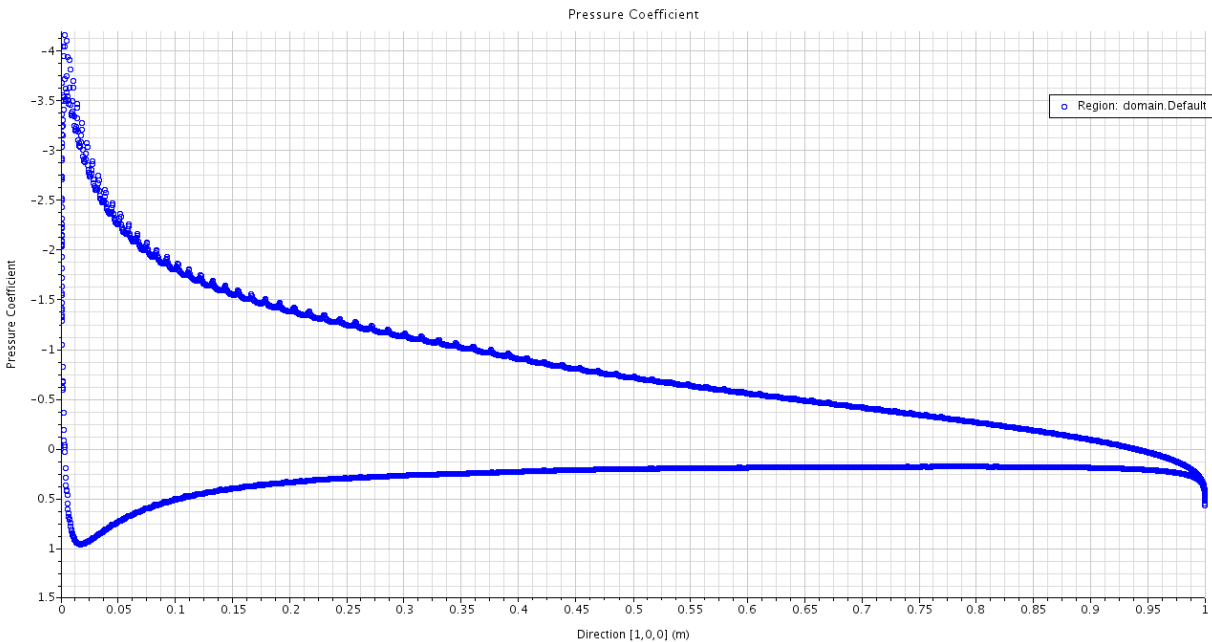


Figure 5: Coefficient of pressure distribution plot for $\alpha = 8$ using Star CCM CFD method.

Therefore, it can be seen that with a larger angle of attack, there will be a greater pressure difference which would create more lift. This trend is consistent with the lift values in Table 1, and shows that until stall occurs.

2.4 Summary

The thin airfoil theory, panel method, and CFD all complete the same task, but with different approaches. Although these various methods do not allow for complete validation of the answers in any individual process (validation can occur only by comparing with real world values), these processes can verify each other in the sense that if the values from each of these processes are similar, then the approach and assumptions used are likely correct for each method.

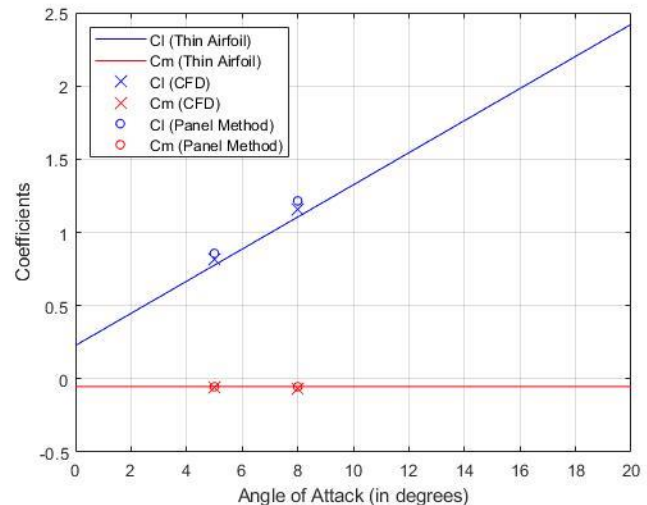


Figure 6: Plot showing coefficients of lift and pitching moment using thin air foil theory, panel method, and CFD.

The coefficients of lift and pitching moment are first to be analyzed. Fig. 6 shows the resulting coefficients of pitching moment and lift using thin air foil method, panel method, and CFD. As can be seen in the figure, each of the three processes resulted in very similar coefficients of pitching moment that remained constant with varying angles of attack. However, the coefficient of lift varied slightly between methods, showing that thin air foil method results in the lowest of the coefficient of lift values, with the panel method results in the largest values.

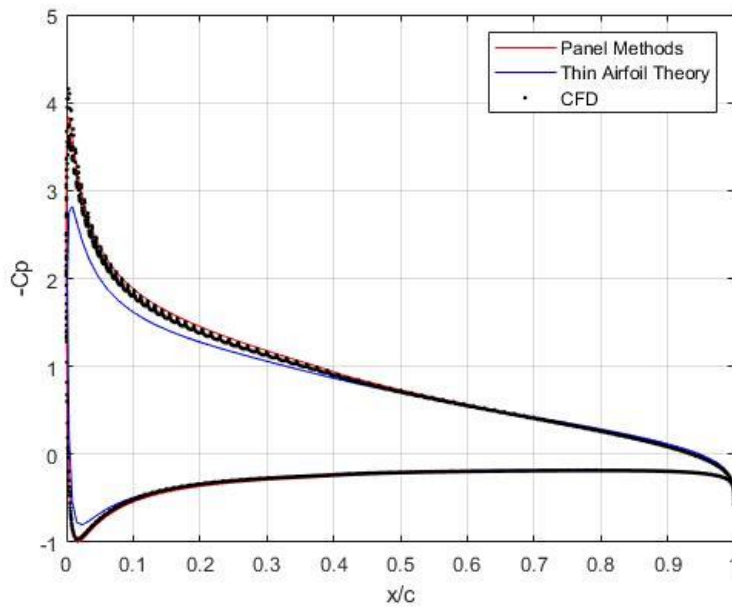


Figure 7: Comparison between the three methods used to find the coefficient of pressure distribution.

The pressure coefficient distributions are then compared for the different processes in Fig. 7. This figure shows that the pressure distributions are very similar between the three different methods with the exception of the thin air foil theory results near the leading edge. This is because the thin air foil theory assumes that only small disturbances exist in the model, which is not true at the leading edge. Therefore, without a correction equation, the coefficient of pressure distribution plot at the leading edge goes to infinity, showcasing one of the main downsides of thin airfoil theory.

As can be seen in Fig. 7, when the Riegel correction is used, the results are more accurate than without the correction since it no longer goes to infinity. However, the result using this correction method is still less accurate than the CFD and panel method results, which emphasizes the limitations of thin air foil method.

Appendix A

Thin Airfoil Theory Matlab Code:

```
clc
clear all

N = 100;

A = 2;
B = 4;
CC = 12;

e = A / 100;
p = B / 10;
t = CC / 100;
phi = linspace(0, pi, N/2+1);
count = 1;

alpha = 8 * (pi/180); % angle of attack in radians

x = 0.5*(1-cos(phi));

[T, ybar, dTdx, dybardx] = naca4(e, p, t, x);

y_up = ybar+T/2;
y_low = ybar-T/2;

x_plot = [flip(x), x(2:end)];
y_plot = [flip(y_low), y_up(2:end)];

% PLOTTING THE AIRFOIL
figure(1)
plot(x_plot, y_plot, 'b')
axis('equal')

% SOLVING FOR THE FOURIER SERIES COEFFICIENTS
A_0 = alpha - (1/pi) * trapz(phi, dybardx);
for R = 1:10
    A_n(R) = (2/pi) * trapz(phi, dybardx.*cos(R*phi));
end

% Calculation for C_ell
m = 2*pi;
alpha_max = 20;
alpha_0 = (1/pi) * trapz(phi, dybardx.*(1-cos(phi)));
X = [0:alpha_max] .* (pi/180); % list of angle of attacks
Y_C_ell = m.*(X-alpha_0);
X_C_ell = [0:alpha_max];

% Calculation for C_mac
Y_C_mac = -pi/4*(A_n(1) - A_n(2));
X_C_mac = [0:alpha_max];
Y_C_mac = Y_C_mac * ones(1,length(X_C_mac));
```

```

% PLOTTING C_ell and C_mac as functions of angle of attack
figure(2)
plot(X_C_ell, Y_C_ell, 'b')
hold on
plot(X_C_mac, Y_C_mac, 'r')
xlabel('Angle of Attack (in degrees)')
ylabel('Coefficients')
legend('Coefficient of Lift', 'Pitching Moment Coefficient',...
      'Location', 'northwest')
grid on

% Calculation for C_p
V_inf = 10; % m/s (freestream velocity)
% compute fourier series coefficients
A_0 = alpha - (1/pi) * ...
      trapz(phi, dybardx); % angle of attack is 8 degrees (C_ell is about 1)

sum = 0;
for R = 1:length(A_n)
    sum = sum + A_n(R)*sin(R.*phi);
end

gamma = 2 * V_inf * ...
      (A_0.*(1+cos(phi))./sin(phi) + sum);

% compute u_c, u_t, v_c, and v_t
dTdx(1) = 0;
q = V_inf .* dTdx;
for R = 1:size(x,2)
    integrand = q./(x(R) - x);
    integrand(R) = 0.0;
    u_t(R) = 1.0/(2*pi).*trapz(x, integrand);
end

for R = 1:size(x, 2)
    integrand = gamma./(x(R)-x);
    integrand(R) = 0.0;
    v_c(R) = -1.0/(2*pi).*trapz(x, integrand);
end
v_c = V_inf.*(dybardx - alpha);

v_t_up = q./ 2.0;
v_t_low = -q./ 2.0;
u_c_up = gamma./ 2.0;
u_c_low = -gamma./ 2.0;

% compute V and V_mod
V_up = sqrt((V_inf*cos(alpha) + u_t + u_c_up).^2 + ...
            (V_inf*sin(alpha) + v_t_up + v_c).^2);

V_low = sqrt((V_inf*cos(alpha) + u_t + u_c_low).^2 + ...
            (V_inf*sin(alpha) + v_t_low + v_c).^2);

```

```

riegel_up = 1./sqrt(1+(dybardx+0.5.*dTdx).^2);
riegel_low = 1./sqrt(1+(dybardx-0.5.*dTdx).^2);

V_mod_up = V_up.*riegel_up;
V_mod_low = V_low.*riegel_low;

C_p_up = 1 - (V_mod_up ./ V_inf).^2;
C_p_low = 1 - (V_mod_low ./ V_inf).^2;

figure(3)
plot(x, -C_p_up, 'b');
hold on
plot(x, -C_p_low, 'b');
grid on
ylim([-1, 1])
xlabel('x/c')
ylabel('-Cp')
% axis('equal')

%-----FUNCTIONS-----
function [T, ybar, dTdx, dybardx] = naca4(e, p, t, x)

    T = 10*t*(0.2969*sqrt(x) - 0.126*x - 0.3536*x.^2 + ...
        0.2843*x.^3 - 0.1015*x.^4);
    dTdx = 10*t*(0.2969*0.5./sqrt(x) - 0.126 - 0.3537*2*x + ...
        0.2843*3*x.^2 - 0.1015*4*x.^3);

    n = length(x);
    ybar = zeros(1, n);
    dybardx = zeros(1, n);

    for i = 1:n
        if x(i) <= p
            ybar(i) = e/p^2 * (2*p*x(i) - x(i)^2);
            dybardx(i) = e/p^2 * (2*p - 2*x(i));
        else
            ybar(i) = e/(1-p)^2 * (1 - 2*p + 2*p*x(i) - x(i)^2);
            dybardx(i) = e/(1-p)^2 * (2*p - 2*x(i));
        end
    end

end

end

```

Appendix B

Panel method Matlab Code:

```

clc
clear all

N = 400;

A = 2;
B = 4;

```

```

CC = 12;
chord = 1;

e = A / 100;
p = B / 10;
t = CC / 100;
phi = linspace(0, pi, N/2+1);
count = 1;
rho = 1.225; % kg/m^3

alpha = 5 * (pi/180); % angle of attack in radians

x = 0.5*(1-cos(phi));

[T, ybar, dTdx, dybardx] = naca4(e, p, t, x);

y_up = ybar+T/2;
y_low = ybar-T/2;

x = [flip(x), x(2:end)];
y = [flip(y_low), y_up(2:end)];

% control points
for R = 1:size(x,2)-1
    x_bar(R) = (x(R) + x(R+1))/2;
    y_bar(R) = (y(R) + y(R+1))/2;
end

% PLOTTING THE AIRFOIL
figure(1)
plot(x, y, 'b')
hold on
plot(x_bar, y_bar, 'xk')
axis('equal')

% Flow tangency boundary condition
V_inf = 10;
for I = 1:N
    theta_i(I) = atan2((y(I+1) - y(I)) , ...
        (x(I+1) - x(I)));

    for J = 1:N
        r_1(I,J) = sqrt((x_bar(I)-x(J+1))^2 + ...
            (y_bar(I)-y(J+1))^2);

        theta_j(J) = atan2((y(J+1)-y(J)) , ...
            (x(J+1) - x(J)));

        r(I,J) = sqrt((x_bar(I)-x(J))^2 + ...
            (y_bar(I)-y(J))^2);
    end
end

```

```

        if I ~= J
            const_1 = x(J)-x_bar(I);
            const_2 = y(J+1)-y_bar(I);
            const_3 = y(J)-y_bar(I);
            const_4 = x(J+1)-x_bar(I);

            beta(I,J) = atan2(((const_1*const_2) - ...
                                (const_3*const_4)) , ...
                                ((const_1*const_4) + ...
                                (const_3*const_2)));
        else
            beta(I,J) = pi;
        end
    end
end

for I = 1:N
    A(I, N+1) = 0.0;
    for J = 1:N
        A(I,J) = log(r_1(I,J)/r(I,J))*sin(theta_i(I)-theta_j(J)) + ...
            beta(I,J)*cos(theta_i(I)-theta_j(J));
        A(I,N+1) = A(I,N+1) + ...
            log(r_1(I,J)/r(I,J))*cos(theta_i(I)-theta_j(J)) - ...
            beta(I,J)*sin(theta_i(I)-theta_j(J));
    end
    b(I) = 2*pi*V_inf*sin(theta_i(I) - alpha);
end

k = 1;
A_k_sum = 0.0;
A_N_sum = 0.0;

% Kutta condition
for J = 1:N
    A_k = beta(k,J)*sin(theta_i(k)-theta_j(J)) - ...
        log(r_1(k,J)/r(k,J))*cos(theta_i(k)-theta_j(J));
    A_N = beta(N,J)*sin(theta_i(N)-theta_j(J)) - ...
        log(r_1(N,J)/r(N,J))*cos(theta_i(N)-theta_j(J));

    A_k_sum = A_k_sum + beta(k,J)*cos(theta_i(k)-theta_j(J)) + ...
        log(r_1(k,J)/r(k,J))*sin(theta_i(k)-theta_j(J));
    A_N_sum = A_N_sum + beta(N,J)*cos(theta_i(N)-theta_j(J)) + ...
        log(r_1(N,J)/r(N,J))*sin(theta_i(N)-theta_j(J));

    A(N+1,J) = A_k + A_N;
end
A(N+1, N+1) = A_k_sum + A_N_sum;
b(N+1) = -2*pi*V_inf * ...
    (cos(theta_i(k)-alpha)+cos(theta_i(N)-alpha));

q_gamma = inv(A)*b'; % solve for source and vortex strengths

% Solve for V_ti
for I = 1:N
    vel_src = 0.0;

```



```

vel_vtx = 0.0;
vel_free = V_inf*cos(theta_i(I)-alpha);

for J = 1:N
    vel_src = vel_src + ...
        q_gamma(J)*(beta(I,J)*sin(theta_i(I)-theta_j(J)) - ...
            log(r_1(I,J)/r(I,J))*cos(theta_i(I)-theta_j(J)));
    vel_vtx = vel_vtx + ...
        q_gamma(N+1)*(beta(I,J)*cos(theta_i(I)-theta_j(J)) + ...
            log(r_1(I,J)/r(I,J))*sin(theta_i(I)-theta_j(J)));
end

V_ti(I) = vel_free + ...
    (1/(2*pi))*vel_src + ...
    (1/(2*pi))*vel_vtx;
end

% Calculate Cp
Cp = 1 - (V_ti/V_inf).^2;
figure(2)
plot(x_bar, -Cp, 'b')
xlabel('x/c')
ylabel('-Cp')

% Calculate Cm
P = 0.5*rho*V_inf^2.*Cp;
for R = 1:N
    F(R) = P(R)*sqrt((x(R+1)-x(R))^2+(y(R+1)-y(R))^2);
    x_dist(R) = 0.25 - x(R); % quarter chord
    y_dist(R) = 0.0 - y(R);
end
F_x = F.*sin(theta_i);
F_y = F.*cos(theta_i);
F = [F_x;F_y;zeros(1,length(F_x))];
distance = [x_dist;y_dist;zeros(1,length(F_x))];

moment = cross(F,distance,2);
moment = moment(:,3);
moment_sum = 0.0;
for R = 1:N
    moment_sum = moment_sum + moment(R);
end

Cm = moment_sum / (0.5*rho*V_inf^2*chord);

% Calculate Cl
gamma_sum = 0;
for R = 1:N
    dist = sqrt((x(R+1)-x(R))^2 + (y(R+1)-y(R))^2);
    gamma_sum = gamma_sum + (q_gamma(end)*dist);
end

lift = rho*V_inf*gamma_sum;
Cl = lift / (0.5*rho*V_inf^2*chord);

```

```

% Calculate Cd
Cd = 0.0; % because drag is 0

%-----FUNCTIONS-----
function [T, ybar, dTdx, dybardx] = naca4(e, p, t, x)

    T = 10*t*(0.2969*sqrt(x) - 0.126*x - 0.3536*x.^2 + ...
        0.2843*x.^3 - 0.1015*x.^4);
    dTdx = 10*t*(0.2969*0.5./sqrt(x) - 0.126 - 0.3537*2*x + ...
        0.2843*3*x.^2 - 0.1015*4*x.^3);

    n = length(x);
    ybar = zeros(1, n);
    dybardx = zeros(1, n);

    for i = 1:n
        if x(i) <= p
            ybar(i) = e/p^2 * (2*p*x(i) - x(i)^2);
            dybardx(i) = e/p^2 * (2*p - 2*x(i));
        else
            ybar(i) = e/(1-p)^2 * (1 - 2*p + 2*p*x(i) - x(i)^2);
            dybardx(i) = e/(1-p)^2 * (2*p - 2*x(i));
        end
    end
end
end

```

Appendix C

Steps outlined in homework memo 1:

To begin, a NACA 2412 airfoil geometry is created using airfoiltools.com and imported into StarCCM. Once imported, the airfoil is extruded 1 meter and the leading and trailing edges are named for convenience. Next, a bullet shaped fluid domain is created around the airfoil following recommended practices for incompressible flow in StarCCM. Mainly, this means that the edge of the domain is 10 body lengths away from the airfoil in all directions. The airfoil is then subtracted from the domain and the back surface is renamed outlet and the other faces are named inlet.

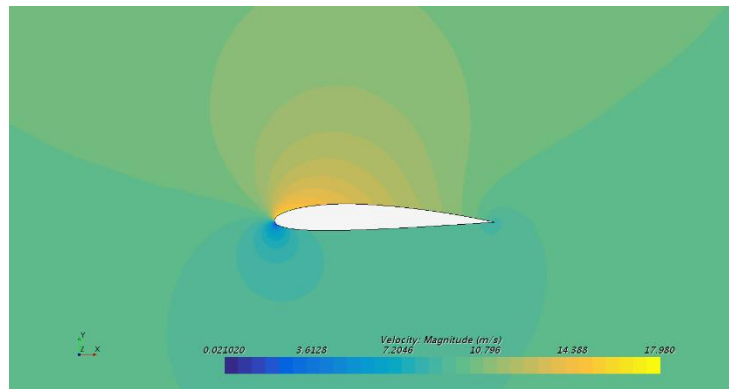


Figure A1: Velocity magnitude plot after stabilization is reached, showing a stagnation point at the leading edge

Once the new part is created, it is assigned as a 2D surface and a mesh is created. This is done according to recommended guidelines as well, resulting in the following parameters:

- Polygonal mesh

- Base size of 1
- Curvature of 72 (1 point to every 5 degrees)
- Surface growth rate of 1.15
- Relative size of 0.1 percentage of base (on le and te)
- Minimum size of 0.05 percent base size (on le and te)

The resulting meshes for different base sizes can be seen in Fig. A2. Next, the physics model is updated. Namely, the model is steady, incompressible, 2D, and not turbulent. Additionally, the domain is set to be a gas with segregated flow and constant density. The velocity is then modeled at a 5° upward slant.

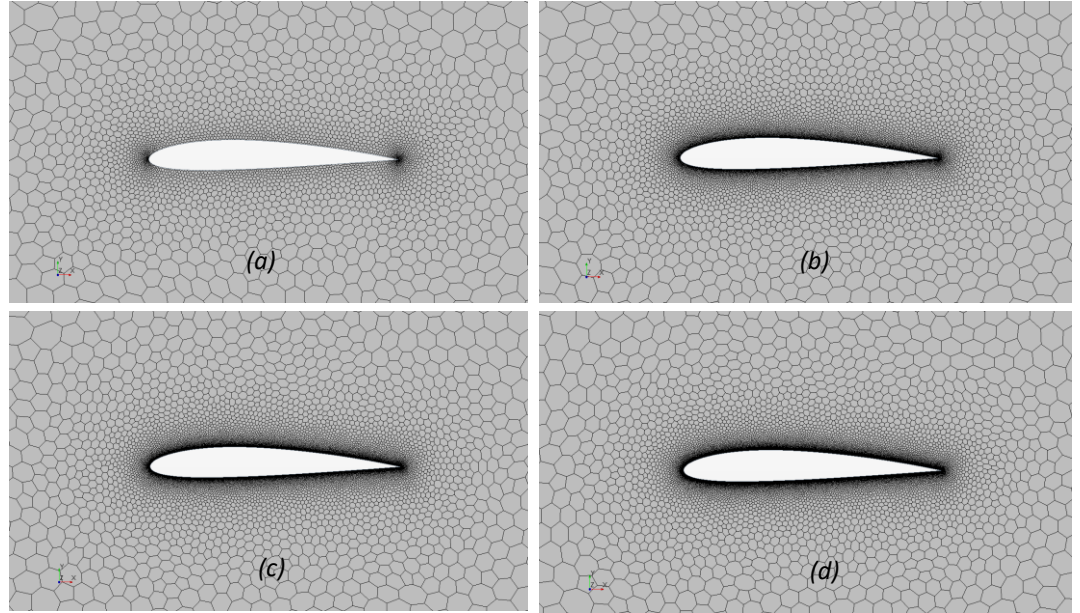


Figure A2: Mesh generations for varying base sizes. As the base size is decreased, the mesh parameters that are relative to the base size become smaller, creating a finer mesh. This is particularly important around the leading and trailing edges for accurate results. (a) Base size=1 (b) Base size=0.1 (c) Base size=0.05 (d) Base size=0.01

Therefore, the initial conditions are set at $v_{ix} = \cos^{-1}(5) * 10$ m/s and $v_{iy} = \sin^{-1}(5) * 10$ m/s.

The inlet regions are then changed so that the velocity inlet matches the 10m/s at a 5° upward slant, as mentioned previously. Additionally, the outlet region is set to zero pressure to create zero pressure drag on the outlet surface. With these parameters in place, reports are created to find the drag and lift, as well as the velocity magnitude via a color bar. The model is then generated and run enough iterations to stabilize and result in a final model as shown in Fig. A3.

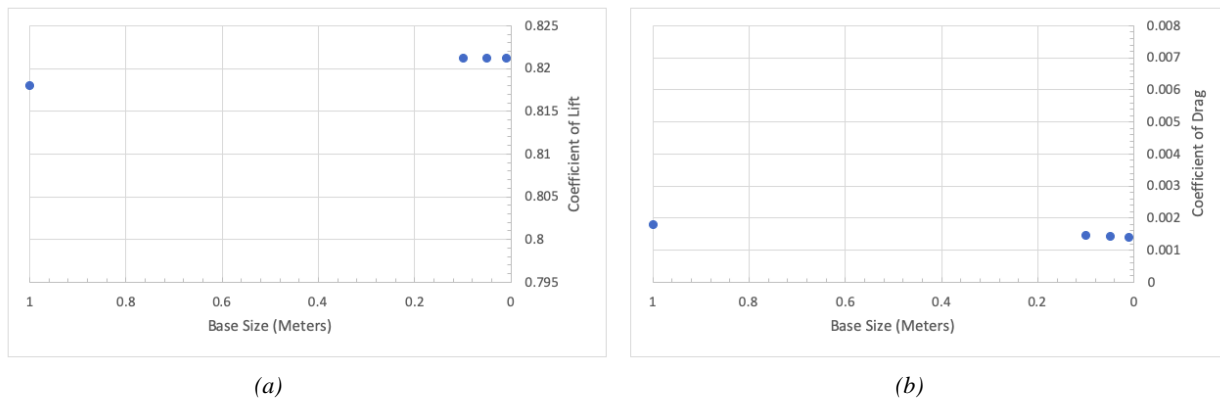


Figure A3: (a) Coefficient of lift vs. base size in meters. The coefficient converges toward the value of 0.821 as base size decreases. (b) Coefficient of drag vs. base size in meters. The coefficient converges toward the value of 0.0014 as the base size decreases.